Pakistan Academy of Sciences

Research Article

Modeling and Technical Analysis of a Modified Z-Source Converter for Driving a Three-Phase Induction Motor

Umar Tabrez Shami[1*], and Zeeshan Lohdi[2]

[1]Electrical Engineering Dept., University of Engineering and Technology, Lahore, Pakistan
[2]Government College of Technology, Abbottabad, Pakistan

Abstract: A modified Z-source converter to boost DC voltage is proposed. The modification has been proposed by engaging an additional power switching device in parallel connection to the conventional Z-source converter. The effectiveness of the additional power switching device in the Z-source converter is demonstrated and discussed in detail. For calculations, a mathematical model of the proposed modified Z-source is also presented. For experimental demonstration the proposed modified Z-source converter is connected to an independent three-phase DC-to-AC three-phase inverter. The load on the modified Z-source converter with a three-phase inverter is a three-phase induction motor. As shown in this paper, the three-phase inverter will play no role boosting the DC voltage. Two well-known PWM switching schemes have been implemented on the three-phase inverter. The proposed modified Z-source converter successfully boosts the DC voltage; in addition, it is shown that the DC output voltage settling time varies with the PWM modulation index.

1. INTRODUCTION

The Z-source converters, originally proposed by Peng [1], demonstrate features normally not found in conventional DC-DC converters. Peng proposed a circuit, connected in-between the source and the main circuit, that presents a single impedance on the source and thus the name Z-source converter. Applications of the Z-source converter include DC-to-AC, AC-to-DC, AC-to-AC, and DC-to-DC power conversion. Many researchers have concentrated on the Z-source converter and proposed improved versions of Z-source controlling methods [2-3], improved Z-source converter control algorithms [4], lowering of stress on semi-conductor power switches used in the Z-source converters [5], and lowering of Z-Source capacitor voltage stress and soft-starting ability [6]. Notably, if a Z-source converter power semi-conductor fails during operation then Gao et al. [7] proposed a reconfigured mode in which the failed power semi-conductor is over passed.

Since the Z-source converter alone can only boost and buck DC voltage, an additional converter is normally required for conversion from DC to AC. Z-source converters can be applied to drive induction motors [8-9], or to drive residential loads as discussed by Huang et al. [10]. Also, Fang et al. [11] proposed a Z-source single phase converter with voltage and power regulation applications. In both, single- and three-phase inverter cases, PWM switching schemes have been used.

This paper demonstrates that the proposed modified Z-source converter is emancipated from a three-phase or single-phase inverter. Simulation results are presented for a modified Z-source converter connected to a three-phase inverter to drive a three-phase motor. The three-phase inverter is switched using two popular PWM switching schemes, i.e., sinusoidal PWM, and trapezoidal PWM scheme. Simulated results include modified Z-source converter input and output voltages, motor terminal voltages, phase current, motor speed, torque, and d-q axis stator
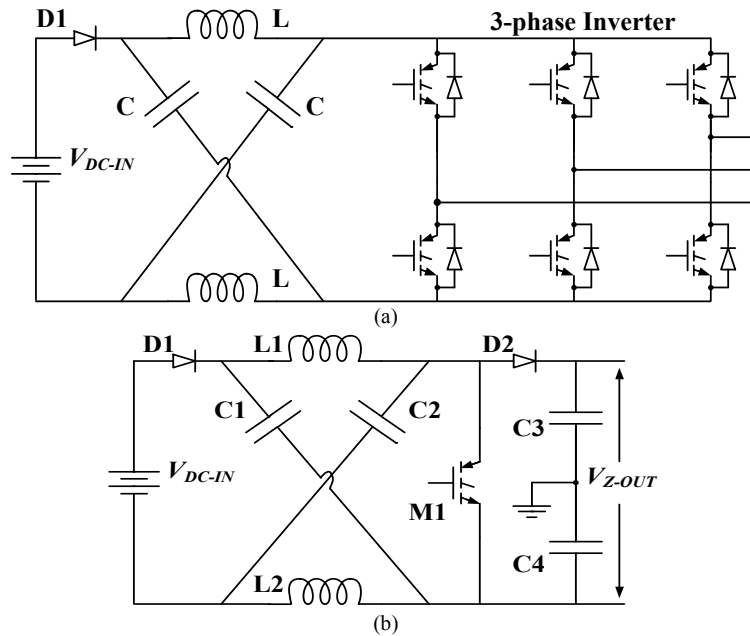
Fig. 1. DC-DC boost circuits: (a) The conventional Z-source converter; (b) Proposed modified Z-source converter.
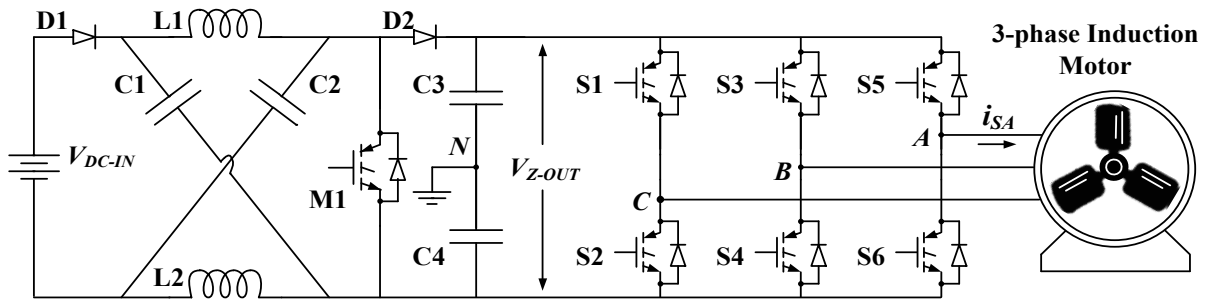

Fig. 2. The proposed modified Z-source converter connected to a three-phase inverter-motor system.

flux trajectories. The results show that the modification introduced to the Z-source converter boost the input voltage and also the output converter voltage is stable. In this paper, technical analysis and discussion is presented on the bases of simulations results.

2. REVIEW OF CONVENTIONAL Z-SOURCE CONVERTER

The conventional Z-source converter, as shown in Fig. 1(a), is an arrangement of two matched inductors and two matched capacitors. This capacitor-inductor network is also called the Z-

source impedance network [1-15]. The Z-source converter functions in two states, i.e., a non-shoot through and a shoot through state. Converters lacking a Z-source impedance network will malfunction if a shoot through state is experienced. The malfunction occurs due to excessive current in the power semi-conductors. With the Z-source impedance in-between the source and load, excessive current may be limited and a malfunction can be prevented. Thus, a shoot through state in Z-source converter is a distinctive feature that is practically implemented with the help of power switching devices. However, the problem lies in the power switching devices that

are performing two tasks, firstly the inverter is controlling the shoot-through and non-shoot-through states of the Z-source converter, and secondly the same power switching devices are transforming DC-to-AC (inverter operation), either single- or three-phase. Hence, there exists a burden on the part of single-or three phase inverters power electronic devices and the switching schemes become complicated to implement [16].

3. THE PROPOSED MODIFIED Z-SOURCE CONVERTER

An interesting circuit proposed by Effah et al. [17], where a Z-source converter is directly connected to a two-level three-phase inverter. The shoot-through and non-shoot through times are implemented by the power switches of the three-phase inverter. Therefore, the power switches perform two types of jobs, firstly implement shoot-through and non-shoot through states for the Z-source converter, and secondly, perform two-level three phase PWM switching.

The proposed modified Z-source converter liberates the three phase inverter from providing shoot-through and non-shoot through states for the Z-source. Fig. 1(b) presents the proposed circuit, where diodes D1 and D2 conduct current only in one direction. Two matched inductors L1, and L2, and two matched capacitors C1, and C2, connected as shown that make the Z-source impedance network. An additional power switching device, M1, is connected across the output of the Z-source inductor capacitor circuit. The power device, M1, will be utilized during shoot-through and non-shoot through states. In addition, M1 can have a duty cycle independent of the switching scheme of the inverter, i.e., M1 can have a long or short shoot- and non-shoot through time. The output voltage of the modified Z-source converter will change with the change in shoot-through and non-shoot through duty times. Following M1 is a diode D2 and two series connected capacitors C3 and C4.

When M1 is switched OFF (switch M1 is open circuited) the Z-source converter is in non-shoot through state and diode D2 will be forward biased thereby, charging both capacitors C3 and C4. On the other hand, when M1 is switched ON (switch M1 is short-circuited) the Z-source converter

undergoes a shoot through state, diode D2 is reversed biased and output voltage of the Z-source is equal to the voltage appearing across the capacitors C3 and C4.

4. PROPOSED MODIFIED Z-SOURCE CONVERTER MATHEMATICAL MODELING

Since, the proposed modified Z-source and the conventional Z-source converter have similar working operation, therefore, the mathematical modeling of the conventional Z-source converter as described in literature [1-17] remain valid for the proposed modified Z-source converter. In the mathematical model to be used here, the output DC voltage, $V_{Z\text{-}OUT}$, of the Z-source is given by,

$$V_{Z-OUT} = \frac{M}{2(2M-1)}V_{DC-IN}, \tag{1}$$

where $V_{DC\text{-}IN}$ is the DC input voltage, M represents the modulation index. In addition, M can be expressed as,

$$M = 1 - (T_O/T) = 1 - D, \tag{2}$$

where T_O represents the duty time of shoot through state, T is the switching time period, and D is the duty cycle. The peak output voltage for any one phase (for example $\hat{v}_{AN}$) can be expressed as,

$$\hat{v}_{AN} = \frac{MB}{2}V_{DC-IN} = \frac{M}{2(2M-1)}V_{DC-IN}, \tag{3}$$

where B represents the boost factor. Note that the boost factor, B, along with the voltage gain G, can be formulated as follows:

$$B = \frac{1}{1 - 2 \cdot T_O/T} = \frac{1}{2M-1}, \tag{4}$$

$$G = MB = \frac{M}{\sqrt{3}M - 1}. \tag{5}$$

Since Z-source capacitors C1 and C2 have the same value, the voltage appearing across individual capacitor i.e., V_{C1} and V_{C2} is given as,

$$V_{C1} = V_{C2} = \frac{B+1}{2}V_{DC-IN}. \tag{6}$$

Likewise, the Z-source inductors L1 and L2 also have similar values and the voltage ripple across individual inductor i.e., ΔV_{L1} and ΔV_{L2}, is expressed as:

$$\Delta V_{L1} = \Delta V_{L2} = \frac{\left(\frac{\sqrt{3}}{2} - \frac{3}{4}\right)M\pi}{3\sqrt{3}M - \pi}V_{DC-IN},\qquad(7)$$

whereas, the current ripple through the inductor becomes,

$$\Delta I_L = \frac{\left(2\sqrt{3} - 3\right)}{24\left(3\sqrt{3}M - \pi\right)}\frac{M\pi V_{DC-IN}}{\omega L}.\qquad(8)$$

The power switches devices, M1, and S1 to S5, are selected on the bases of maximum working voltage, V_{Z-OUT}, and the maximum current capacity, I_{MAX}. The maximum momentary output power, P_{MAX}, and normal output power, $P_{AVG,}$ assist in determining the maximum current I_{MAX}, i.e.,

$$I_{MAX} = \frac{P_{MAX}/2}{V_{CAP}} + 2I_L = \frac{P_{MAX}/2}{V_{CAP}} + 2\frac{P_{AVG}}{V_{DC-IN}}.\qquad(9)$$

5. SIMULATION SETUP

Computer software Matlab-Simulink® based simulations have been conducted to test the modified Z-source converter. Fig. 2 presents the circuit diagram of this modified Z-source converter connected to a three-phase inverter-motor system. The inverter is switched according to two well-known switching schemes [18-19], which are:

1) Sinusoidal PWM (SPWM), and

2) Trapezoidal PWM (TPWM).

No alterations have been adopted while using SPWM and TPWM schemes. The self-governing operation of the modified Z-source converter is demonstrated by switching the three-phase inverter according to the two above mentioned switching schemes, consecutively. With the help of mathematical modeling shown from (1) to (9), the modified Z-source converter simulation model is designed with the following parameters.

i.   Input DC voltage V_{DC-IN} = 64 V.

ii.   Z-source network: L1=L2=10 µH; C1=C2=15 µF.

iii. Filter Capacitors: C3=C4=100µF.

iv.   Switching power devices, M1, and S1 to S5: IGBT(Model:IRFP460)

v.   Z-source Switching frequency=10 kHz.

vi.   Z-source duty cycle: D=60%.

vii. Induction motor: three-phase 400V, 4 kW.

viii. Load torque presented on the motor T_L = 10 Nm.

5.1 Three-phase Induction Motor Model

The induction motor or asynchronous machine model as found in Matlab-Similink™ library, and shown in fig. 3(a), is a standard machine model that operates in generator or motor configuration. The electrical quantities including resistance, inductances (useful and leakage) are all transferred to the stator side. A fourth-order state space model is used to represent the electrical parts of the induction motor e.g., stator and rotor voltages and currents. Whereas a second-order model represents the mechanical part of motor, e.g., torque and speed. While in motor configuration Tm, i.e., the torque, is set to positive and a constant number is assigned to set the value of torque. In addition, three-phase input voltage is provided to the motor model. The motor output parameter e.g., motor phase current, motor speed, are observed with the help of output box [20].

A standard induction motor model as provided by the simulation software Matlab-Similink™ is used. Using the model within the set voltage and torque level, will abstain the motor from entering the unstable region.
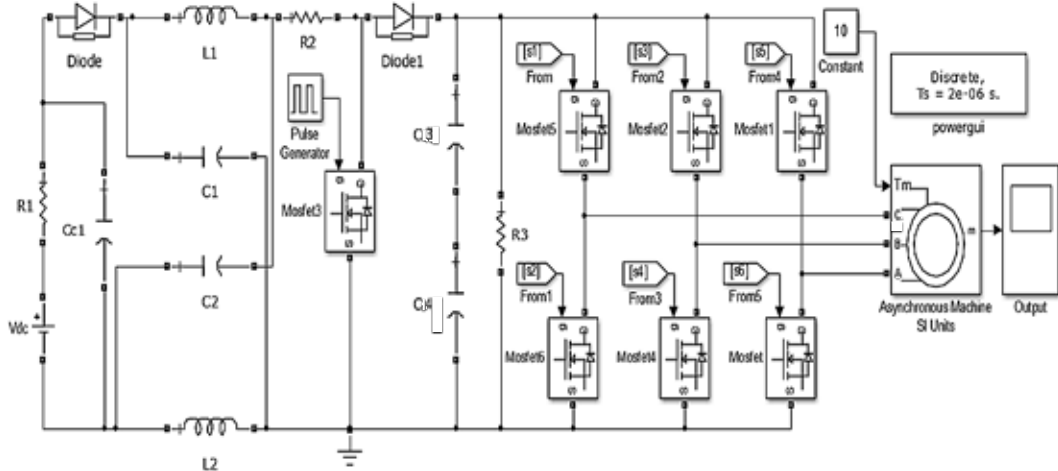
The induction motor phase voltages and phase currents can be transformed into the quadratic (d-q axis) reference frame as follows. For the voltages,

$$\begin{bmatrix} v_d \\ v_q \end{bmatrix} = \frac{2}{3}\begin{bmatrix} 1 & -\frac{1}{2} & -\frac{1}{2} \\ 0 & -\frac{\sqrt{3}}{2} & \frac{\sqrt{3}}{2} \end{bmatrix}\begin{bmatrix} v_{AB} \\ v_{BC} \\ v_{CA} \end{bmatrix},\qquad(10)$$
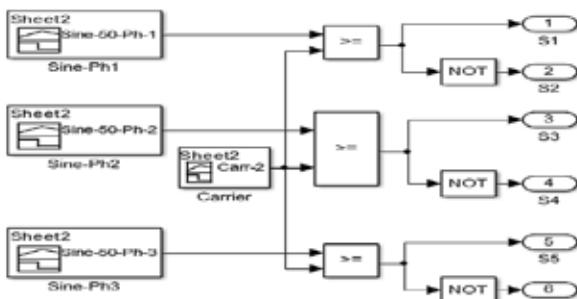
where v_{AB}, v_{BC}, v_{CA} are the instantaneous phase voltages; v_d, and v_q, are the transformed voltages in the d-axis and q-axis, respectively. Similarly, for the currents,

$$\begin{bmatrix} i_d \\ i_q \end{bmatrix} = \frac{2}{3}\begin{bmatrix} 1 & -\frac{1}{2} & -\frac{1}{2} \\ 0 & -\frac{\sqrt{3}}{2} & \frac{\sqrt{3}}{2} \end{bmatrix}\begin{bmatrix} i_{SA} \\ i_{SB} \\ i_{SC} \end{bmatrix},\qquad(11)$$
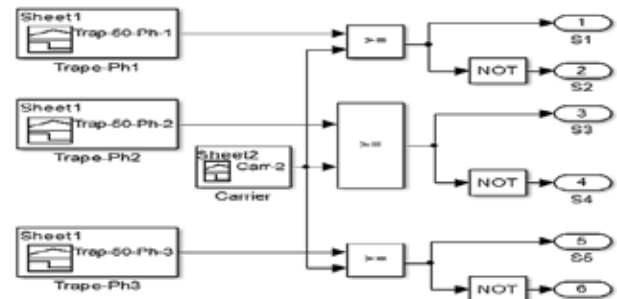
i_{SA}, i_{SB}, and i_{SC}, are the instantaneous stator currents whereas i_d, and i_q, are the transformed currents in the d-axis and q-axis, respectively.
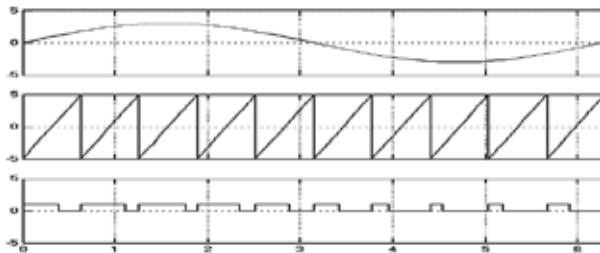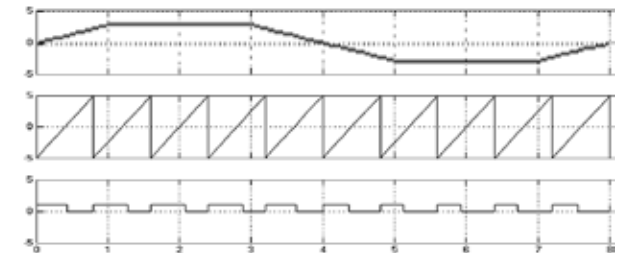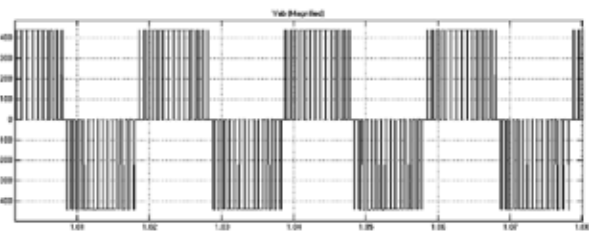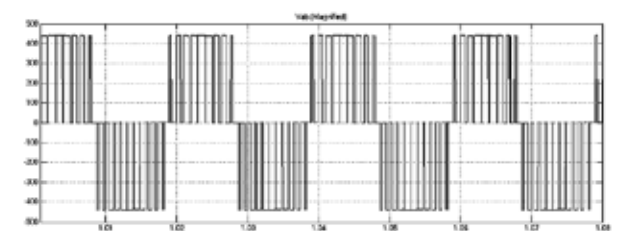
(a)

(b)

(c)

(d)

(e)

(f)

(g)

Fig. 3. The simulation model: (a) Simulation of proposed circuit; (b) Simulation model diagram of Sinusoidal PWM scheme; (c) Simulation model diagram of Trapezoidal PWM scheme; (d) Sinusoidal, Carrier waves and the PWM switching sequence scheme; (e) Trapezoidal, Carrier waves and the PWM switching sequence scheme; (f) Output voltage of the Sinusoidal PWM inverter; (g) Output voltage of the Trapezoidal PWM inverter.
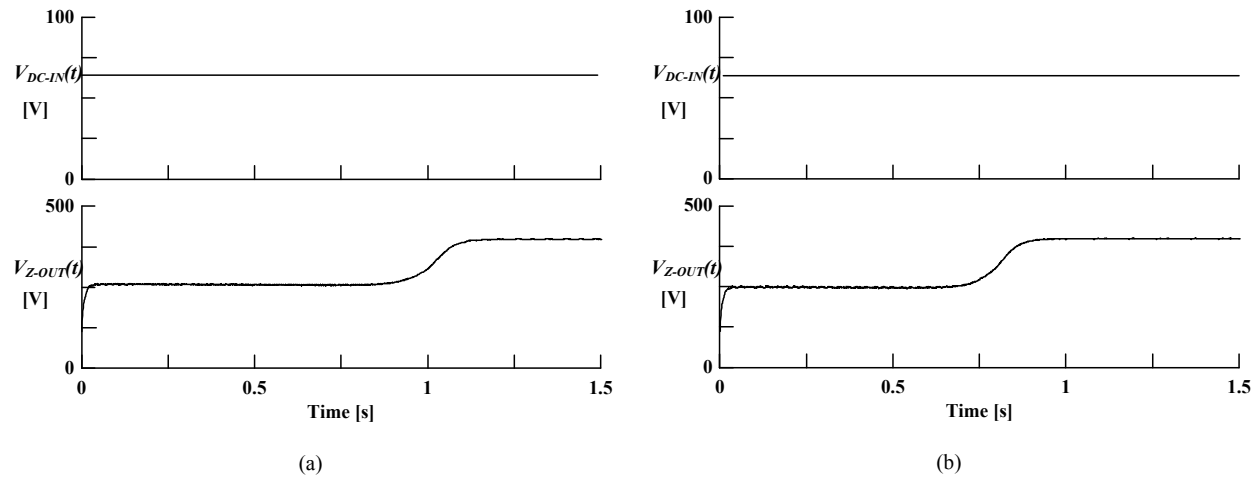
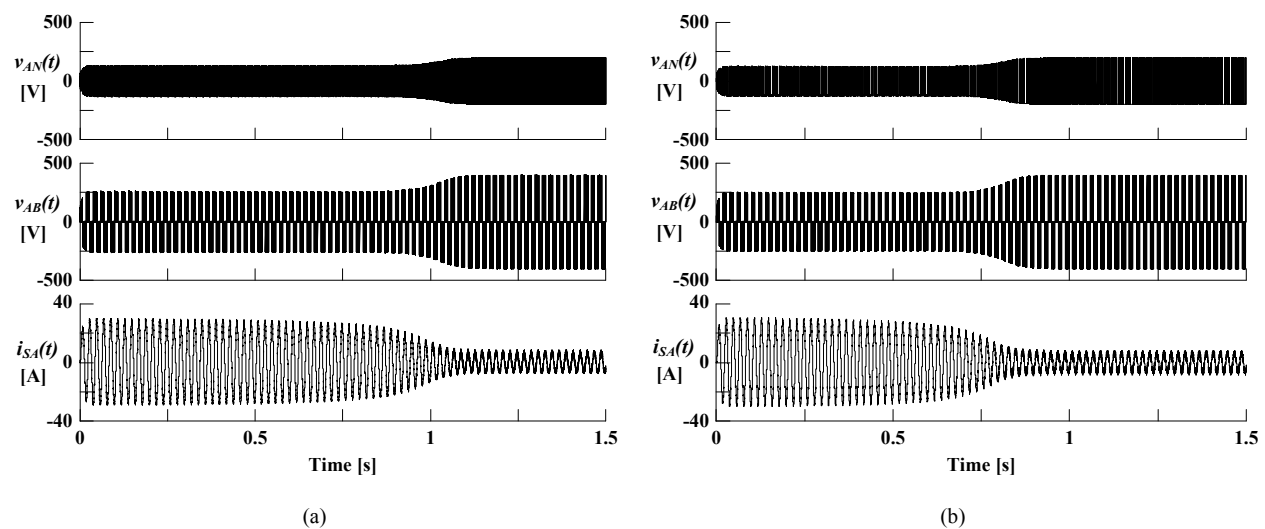**Fig. 4.** The modified Z-source converter input and output voltage for: (a) SPWM; and (b) TPWM.

Fig. 5. The induction motor phase-to-neutral, phase-to-phase voltage, and stator current for: (a) SPWM; and (b) TPWM.
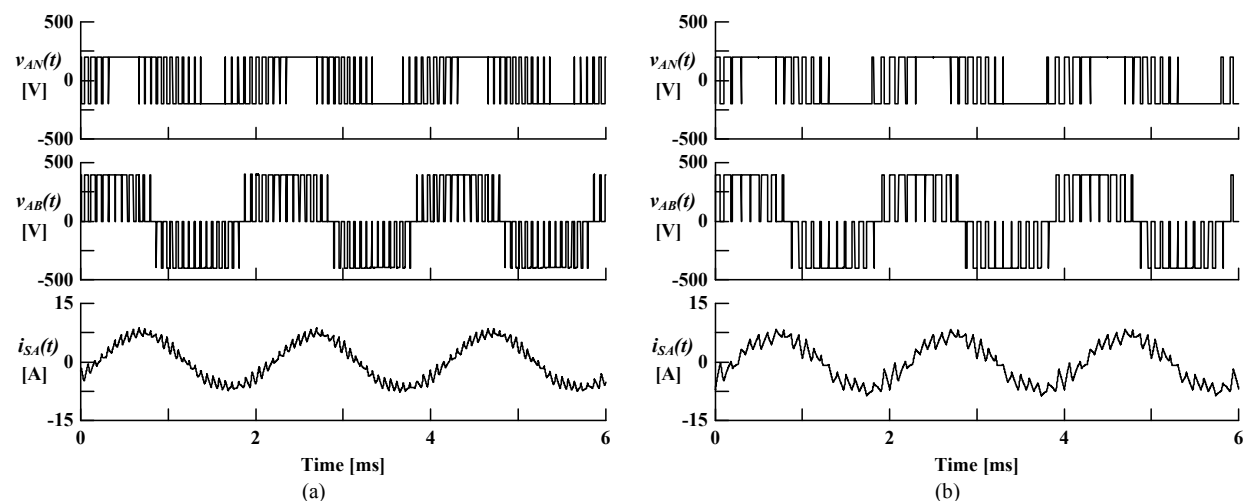
Fig. 6. Time expanded induction motor phase-to-neutral, phase-to-phase voltage, and stator current for: (a) SPWM; and (b) TPWM.

5.2 Control Scheme of Sinusoidal and Trapezoidal PWM

The control schemes to implement sinusoidal and trapezoidal PWM, are shown in Fig. 3(b) and Fig. 3(c), respectively. In each case, a reference signal (either sinusoidal or trapezoidal) is compared with a carrier signal; the result of the comparison generates a PWM signal from outputs S1 to S6. Whereas, the reference, carrier, and output signal for sinusoidal and trapezoidal PWM, are displayed in Fig. 3(d) and Fig. 3(e), respectively. The inverter phase-to-phase voltage for sinusoidal and trapezoidal PWM, are shown in Fig. 3(f) and Fig. 3(g), respectively. Feedback control is beyond the scope of this research; hence the system is kept in open loop system.

6. SIMULATION RESULTS

The following parameters are extracted from the simulation results for analysis, i.e.,

a. Input DC voltage, V_{DC-IN}
b. Z-source Output DC voltage, V_{Z-OUT}
c. Phase-to-neutral voltage (for any one phase, e.g., phase a) $v_{AN}(t)$
d. Phase-to-phase voltage (for any two phases) $v_{AB}(t)$
e. Stator phase current (for any one phase) $i_{SA}(t)$
f. Induction motor speed curve.
g. Induction motor torque curve.
h. Stator flux on the d-q axis.

6.1 Z-Source Converter Input and Output Voltage

The required output voltage from the modified Z-source converter is 400V. To obtain this voltage the switching frequency and duty cycle are set to 10kHz and 60%, respectfully. The modified Z-source converter input (V_{DC}) and output voltage (V_{Z-OUT}) for SPWM and TPWM, are presented in Fig. 4(a) and Fig. 4(b), respectively. The input voltage is a constant DC voltage of 64V and the steady-state output voltage is 400V. The transient time for Z-source converter when running with sinusoidal PWM scheme is observed to be longer than that of trapezoidal PWM scheme.

6.2 Induction Motor Voltages and Currents

The induction motor voltages and currents for SPWM and TPWM are shown in Fig. 5. Here,

$v_{AN}(t)$ represents motor phase-to-neutral voltage, $v_{AB}(t)$ represents motor phase-to-phase voltage, $i_{SA}(t)$ represents the stator current in phase A. Comparing Fig. 5(a) and Fig. 5(b), the phase-to-neutral voltage and phase-to-phase voltage require a longer settling time in the case of SPWM than TPWM. Also, the starting current for stator current $i_{SA}(t)$ last longer in the case SPWM than for TPWM. Fig. 6 demonstrates the time-expanded waveforms for $v_{AN}(t)$, $v_{AB}(t)$, and $i_{SA}(t)$. The peak-to-peak ripple-current value for $i_{SA}(t)$ in case for SPWM is smaller than peak-to-peak ripple-current for TPWM. Fig. 7(a) and Fig. 7(b) displays the frequency analysis of motor phase-to-neutral voltage (RMS) V_{AN}, motor phase-to-phase voltage V_{AB}, stator current in phase A, I_{SA}, for SPWM and TPWM, respectively. Ignoring higher order of harmonics, the frequency analysis for both SPWM and TPWM are very much similar. On the other hand, the total harmonic distortion (THD) in terms of phase to neutral and phase to phase voltages, of TPWM is less when compared to THD of SPWM. Table I presents a comparison of THD in motor voltages and current for SPWM and TPWM schemes. Table 2 presents a summary of three-phase inverter driven motor system characteristics with modified Z-source converter.

Table 1. Comparison of the in Motor Voltages and Current for SPWM and TPWM.

Motor parameter	SPWM (%)	TPWM (%)
Phase to neutral voltage, v_{AN}	93.92	81.89
Phase voltage, v_{AB}	65.34	60.03
Stator current, i_{SA}	15.91	23.83

Table 2. Three-Phase Inverter Driven Motor System Characteristics with Modified Z-source converter.

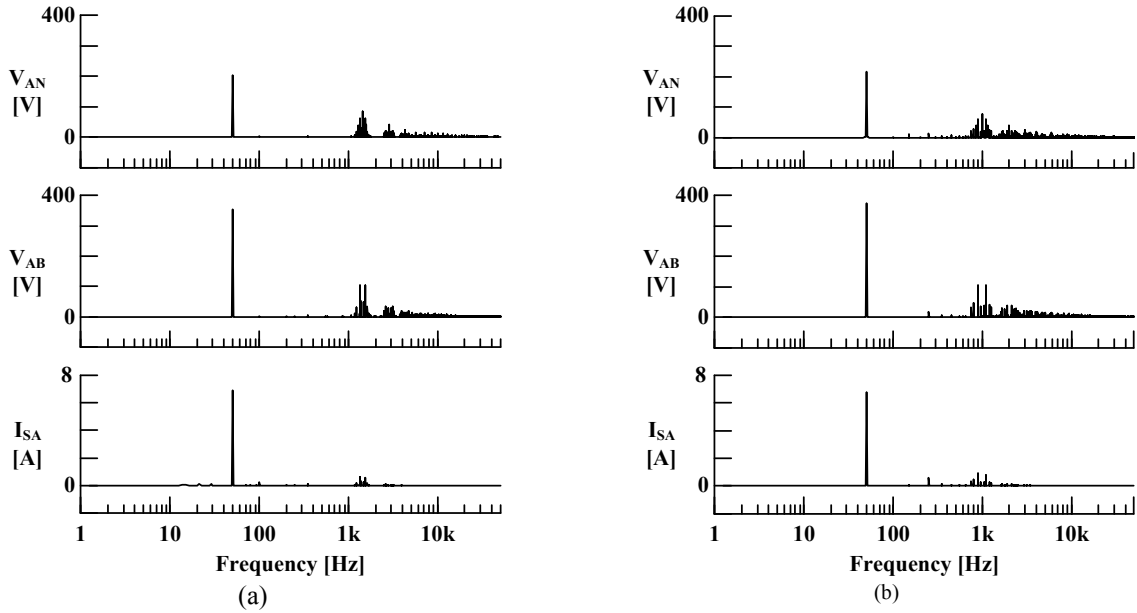| Parameter	Switching Schemes		Units
	SPWM	TPWM	
V_{DC-IN}	63.98	63.98	V
V_{Z-OUT}	397.9	397.9	V
Power switch M1 switching frequency	10k	10k	Hz
Output DC voltage settling time	1.1	0.892	s
V_{AN}	198.6	198.6	V
V_{AB}	299.3	308.7	V
I_{SA}	4.949	4.935	A
Motor Speed	150.3	151.1	RPM
Motor Torque	10.44	10.45	N.m

Fig. 7. Frequency analysis of induction motor phase-to-neutral, phase-to-phase voltage, and stator current for: (a) SPWM; and (b) TPWM.
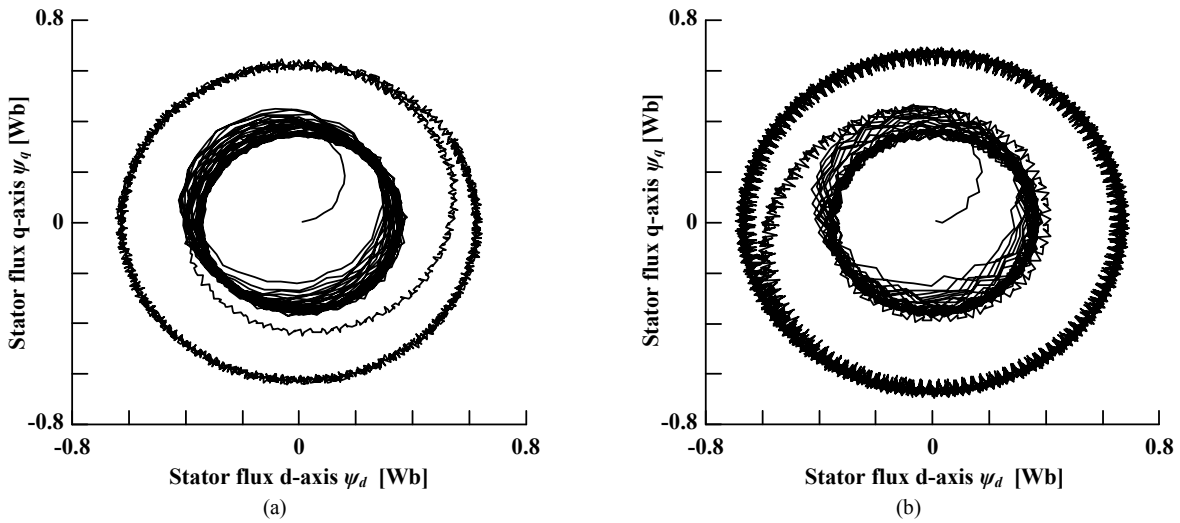

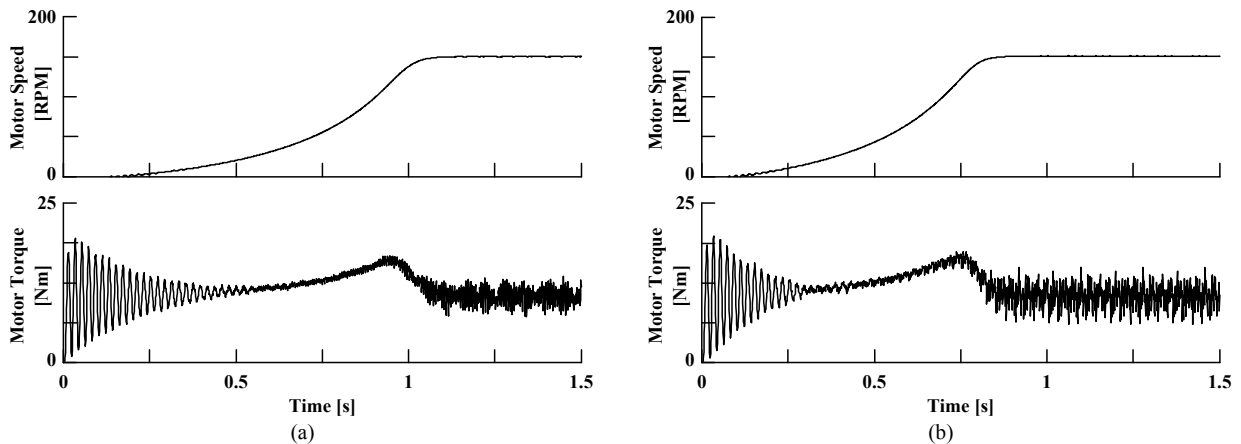**Fig. 8.** The d-q axis stator flux trajectories for: (a) SPWM; and (b) TPWM.

Fig. 9. Induction motor speed and torque for: (a) SPWM; and (b) TPWM.

7. DISCUSSION

The conventional Z-source converter, although equipped with less number of power switches, may face problems such as error in non-shoot through mode due to dead time of the power switches, as described earlier Gao et al. [7]. The application of a separate power switch (M1) as proposed here in the modified Z-source converter has brought flexibility, both to the Z-source and the three-phase inverter.

With an inverter driven motor connected to the modified Z-source converter, it is observed in Fig. 4 and 5, the settling time required to achieve a steady DC output voltage in the case of SPWM is longer i.e., approximately 1.1s, as compared to TPWM case which is approximately 0.89s. In this context an investigation of Fig. 6, suggests that modified Z-source converter takes a shorter time to settle the output DC voltage while operating under the TPWM scheme which can be related to the number of PWM pulses present in one cycle for TPWM being less than those present in SPWM scheme.

Additionally, as shown in Fig. 6, the SPWM scheme produces less stator peak-to-peak ripple current compared to TPWM, it is because the PWM pulse count in SPWM is larger than TPWM. The duty cycle of individual PWM pulses in SPWM is smaller than those present in TPWM case. Therefore, with SPWM the stator current faces smaller time to flow and smaller time to stop flowing. Furthermore, with reference to Fig. 7, the frequency analysis of stator current i.e., I_{SA} for SPWM and TPWM, it is observed that harmonics content in TPWM have larger amplitude compared to those of SPWM.

The d-q axis stator flux trajectories as produced by SPWM and TPWM are shown in Fig. 8(a) and Fig. 8(b), respectively. For both SPWM and TPWM cases, each d-q axis trajectory consists of an inner and an outer trajectory loop. The inner trajectory loop is created during the starting time i.e., when the modified Z-source converter output DC voltage is in transient (non-steady) state. Likewise, the outer trajectory loop is created when output DC voltage is steady. An ideal d-q axis stator flux trajectory is a regular ripple free circular path. Since the motor is fed from an inverter that is producing PWM waveforms, therefore voltages presented at the motor terminals are non-sinusoidal and the d-q axis stator flux trajectory experiences flux ripples. The

dependency of flux on motor voltage and current can be derived. The induction motor stator flux, ψ, and the d-q axis flux, ψ_d and ψ_q, [21] are related as follows:

$$\psi = \sqrt{\psi_d^2 + \psi_q^2} \tag{12}$$

With the help of (10) and (11), the d-q axis flux can be represented in terms of d-q axis voltages and current as, for ψ_d, and for ψ_q,

$$\psi_d = \int (v_d - R_s i_d) dt \tag{13}$$

$$\psi_q = \int (v_q - R_s i_q) dt \tag{14}$$

where R_S in both eqs. (13) and (14), is the stator resistance. Therefore, a comparison of phase voltage and stator current shown in Fig. 6 to d-q axis flux of SPWM and TPWM shown in Fig. 8, becomes clear to understand. That is, the d-q axis stator flux trajectory for SPWM has less flux ripple as compared to flux ripple for TPWM.

Fig. 9(a) and Fig. 9(b) present induction motor speed and torque for SPWM and TPWM case, respectively. It is noted that the induction motor settles to a steady speed and torque, in a less amount of time in the case of TPWM as compared to SPWM. According to the results, the motor settles to the required speed and torque in a shorter time, almost 0.98s in the case of TPWM as compared to SPWM which approximately takes 1.1s to settle. It is also observed that the peak to peak torque ripple in the case of TPWM is greater than that of SPWM case. In addition, results also show that the average motor torque ripple of the SPWM inverter us 2.7% less than that produced in TPWM inverter. The induction motor torque, T, in terms of d-q frame of reference parameters, ψ_d, ψ_q, i_d, and i_q, can then be represented as [22-23],

$$T = \frac{3}{2} p (\psi_d i_q - \psi_q i_d) . \tag{15}$$

where p is the number of pole pairs. Results obtained are consistent with (15), since peak to peak flux ripple the case of TPWM is greater than that on SPWM, resulting in a greater torque ripple in TPWM case.

8. CONCLUSIONS

This paper has presented a modified Z-source converter by installing an additional power switching device to the output of the conventional

Z-source converter. The proposed Z-source converter boosts the DC voltage without the need of three-phase inverter power switches. However, a three-phase inverter is used to drive a three-phase motor. Compared to the conventional Z-source converter that requires at least two power switching devices to operate, the proposed modified Z-source converter requires only one power switching device. This exclusive feature of the proposed Z-source converter can be useful for a range of DC–AC, AC–DC, AC–AC, and DC–DC power transformations. The proposed modified Z-source converter is tested in simulations. The modified Z-source converter has successfully boosted an input DC voltage of 64V to 400V. The output voltage of the modified Z-source converter is connected to a three-phase inverter to drive a three-phase induction motor. Two well-known PWM techniques to switch the three-phase inverter are adopted. Although the individual PWM switching schemes applied to the three-phase inverter, effect the settling time of the output DC voltage, but do not control the voltage gain of the modified Z-source converter. The SPWM takes more rotor speed settle time and longer starting current but once settled the d-q currents and torque ripple are both less. The TPWM takes less rotor speed settling time, a shorter starting current but after settling the d-q currents and torque ripple are large as compared to SPWM. The simulation results have shown satisfactory performance of the proposed modified Z-source converter for electrical engineering applications.

9. REFERENCES

1. Peng, F.Z. Z-source inverter. *IEEE Transactions on Industry Applications.* 39(2): 504-510 (2003).
2. Shen, M., J. Wang, A. Joseph, F. Z. Peng, L. M. Tolbert, & D. J. Adams. Constant boost control of the Z-source inverter to minimize current ripple and voltage stress. *IEEE Transactions on Industry Applications* 42(3): 770-778 (2006).
3. Jung, J.W., & A. Keyhani. Control of a Fuel Cell Based Z-Source Converter. *IEEE Transactions on Energy Conversion* 22(2): 467-476 (2007).
4. Tran, Q.V., T. W. Chun, J. R. Ahn, & H. H. Lee. Algorithms for Controlling Both the DC Boost and AC Output Voltage of Z-Source Inverter. *IEEE Transactions on Industrial Electronics* 54(5): 2745–2750 (2007).
5. Evran, F., & M.T. Aydemir. Z-source-based isolated high step-up converter. *IET Power Electronics* 6(1): 117-124 (2013).

6. Tang, Y., S. Xie, C. Zhang, & Z. Xu. Improved Z-source inverter with reduced Z-source capacitor voltage stress and soft-start capability. *IEEE Transactions on Power Electronics* 24(2): 409-415 (2009).
7. Gao, F., P. C. Loh, F. Blaabjerg, & D. M. Vilathgamuwa. Performance evaluation of three-level Z-source inverters under semiconductor-failure conditions. *IEEE Transactions on Industry Applications* 45(3): 971-981 (2009).
8. Peng, F.Z., X. Yuan, X. Fang, & Z. Qian. Z-source inverter for adjustable speed drives. *IEEE Power Electronics Letters* 1(2): 33-35 (2003).
9. Peng, F.Z., A. Joseph, J. Wang, M. Shen, L. Chen, Z. Pan, E. O. Rivera, & Y. Huang. Z-source inverter for motor drives. *IEEE Transactions on Power Electronics* 20(4): 857-863 (2005).
10. Huang, Y., M. Shen, F. Z. Peng, & J. Wang. Z-source inverter for residential photovoltaic systems. *IEEE Transactions on Power Electronics* 21(6): 1776-1782 (2006).
11. Fang, X.P., Z.M. Qian, & F.Z. Peng. Single-phase Z-source PWM AC-AC converters. *IEEE Power Electronics Letters* 3(4): 121-124 (2005).
12. Shen, M. J., Wang, A. Joseph, F. Z. Peng, L. M. Tolbert, & D. J. Adams. Maximum constant boost control of the Z-source inverter. *Industry Applications Conference. 39th IAS Annual Meeting. Conference Record of the 2004 IEEE* p. 142-147 (2004).
13. Sack, L., B. Piepenbreier, & M. V. Zimmermann. Dimensioning of the Z-source inverter for general purpose drives with three-phase standard motors. In: *IEEE Power Electronics Specialists Conference,* p. 1808-1813 (2008).
14. Sack, L., B. Piepenbreier, & M. V. Zimmermann. Z-source inverter for general purpose drives in motoring and regenerating operation. *Proceedigns of International Symposium on Power Electronics, Electrical Drives, Automation and Motion, SPEEDAM.* p. 766-771 (2008).
15. Rajakaruna, S. & L. Jayawickrama. Steady-state analysis and designing impedance network of Z-source inverters. *IEEE Transactions on Industrial Electronics* 57(7): 2483-2491 (2010).
16. Kim, S., J. Park, K. Lee, & T. Kim. Novel pulse-width modulation strategy to minimize the switching losses of Z-source inverters. *Electric Power Components and Systems* 42(11): 1213-1225 (2014).
17. Effah, F. B., P. Wheeler, J. Clare, & A. Watson. Space-vector-modulated three-level inverters with a single Z-source network. *IEEE Transactions on Power Electronics* 28(6): 2806-2815 (2013).
18. Rashid, M.H. *Power Electronics: Circuits, Devices and Applications*, 4th ed., Prentice Hall, NJ (2013).
19. Shami, U.T., & T.A. Shami. An evaluation of approximated PWM switching schemes instigating

acoustic noise in inverter-fed induction motors. *Proceedings of the Pakistan Academy of Sciences A. Physical and Computational Sciences* 53 (3): 319–324 (2016).

20. MATHWorks ™ documentation library [online] https://www.mathworks.com/help/physmod/sps/po wersys/ref/ asynchronousmachine.html (Accessed 14 February, 2017).

21. Zhang, Z., R. Tang, B. Bai, & D. Xie. Novel direct torque control based on space vector modulation with adaptive stator flux observer for induction motors. *IEEE Transactions on Magnetics* 46(8): 3133-3136 (2010).

22. Habetler, T.G., F. Profumo, M. Pastorelli, & L.M. Tolbert. Direct torque control of induction machines using space vector modulation. *IEEE Transactions on Industry Applications* 28(5): 1045-1053 (1992).

23. Kouro, S., R. Bernal, H. Miranda, C. A. Silva, & J. Rodríguez. High-performance torque and flux control for multilevel inverter fed induction motors. *IEEE Transactions on Power Electronics* 22(6): 2116-2123 (2007).